

Changes in opal flux and the rain ratio during the last 50,000 years in the equatorial Pacific

Mathieu Richaud^{a,*}, Paul Loubere^a, Sylvain Pichat^{b,2}, Roger Francois^c

^aDepartment of Geology and Environmental Geosciences, Northern Illinois University, DeKalb, IL 60115, USA

^bEarth Sciences Department, University of Oxford, Oxford, UK

^cDepartment of Earth and Ocean Sciences Oceanography, University of British Columbia, Vancouver, BC, Canada

Accepted 12 January 2007

Available online 16 March 2007

Abstract

Changes in the orgC/CaCO₃ ratio in particles sinking from the surface to the deep ocean have the potential to alter the atmospheric pCO₂ over the span of a glacial/interglacial cycle. Recent paleoceanographic and modern observational studies suggest that silica is a key factor in the global carbon biogeochemical cycle that can influence the flux ratio, especially at low latitudes, through “silicic acid leakage” [Brzezinski, M., Pride, C., Franck, M., Sigman, D., Sarmiento, J., Matsumoto, K., Gruber, N., Rau, R., Coale, K., 2002. A switch from Si(OH)₄ to NO₃⁻ depletion in the glacial Southern Ocean. *Geophysical Research Letters* 29, 5]. To test this hypothesis, we reconstruct biogenic fluxes of CaCO₃, orgC and Si for three equatorial Pacific cores. We find evidence that a floral shift from a SiO₂-based community to a CaCO₃-based occurred, starting in mid-marine isotope stage (MIS) 3 (24–59 cal. ka) and declining toward MIS 2 (19–24 cal. ka). This could reflect the connection of the Peru upwelling system to the subantarctic region, and we postulate that excess silica was transported from the subantarctic via the deep Equatorial Undercurrent to the eastern equatorial Pacific. In the eastern equatorial Pacific only, we document a significant decrease in rain ratio starting mid-MIS 3 toward MIS 2. This decrease is concomitant with a significant decrease in silica accumulation rates at the seabed. This pattern is not observed in the Pacific influenced by equatorial divergence and shallow upwelling, where all reconstructed fluxes (CaCO₃, orgC, and opal) increase during MIS 2. We conclude that the overall calcium carbonate pump weakened in the EEP under Peru upwelling influence.

© 2007 Elsevier Ltd. All rights reserved.

Keywords: Equatorial Pacific

1. Introduction

Bubbles of ancient air trapped in Antarctic ice reveal that atmospheric pCO₂ during glacials was

80–90 p.p.m.v. lower than the pre-anthropogenic interglacial value of 280 p.p.m.v. (Petit et al., 1999). Numerous studies have highlighted the importance of pCO₂ as an amplifier and/or primary driver of the glacial cycles. However, we remain ignorant of the mechanisms responsible for the glacial/interglacial CO₂ cycles (Archer et al., 2000; Sigman and Boyle, 2000). One viable hypothesis for the cause of glacial/interglacial CO₂ change involves the extraction of carbon from the surface ocean by biological

*Corresponding author. Tel.: +1 815 501 8149.

E-mail address: mathieu@geol.niu.edu (M. Richaud).

¹Now at Department of Geology and Geography, Georgia Southern University, Statesboro, GA 30458, USA.

²Now at Laboratoire de Sciences de la Terre, Ecole Normale Supérieure de Lyon, Lyon, France.

production, either at low or high latitudes, coupled with changes in the marine calcium carbonate and silica budgets (Archer et al., 2000; Sigman and Boyle, 2000). Biological production plays a significant role in modulating CO₂ release from the ocean to the atmosphere and transferring carbon to the deep-ocean reservoirs by producing biogenic particles (i.e., organic carbon, calcite, and opal). The two most important regions of the ocean for exchange of CO₂ with the atmosphere are the equatorial Pacific and the Southern Ocean; the former is a net source and the latter is a net sink under present conditions. Because the equatorial Pacific is the site of the greatest evasion of CO₂ (0.8–1.0 Pg C year⁻¹ from the modern oceans; Takahashi et al., 2002), it may have played a role in glacial/interglacial changes in atmospheric pCO₂ (Palmer and Pearson, 2003).

In the Southern Ocean, it has been demonstrated that phytoplankton productivity could be limited by the availability of iron as shown by iron fertilization experiments in this area (Boyd et al., 2000; Buesseler et al., 2004). It was also noted that the addition of Fe consistently favors diatoms over other phytoplankton (Coale et al., 1996). This led Brzezinski et al. (2002) to propose the “silicic acid leakage” hypothesis to explain the changes in atmospheric CO₂ recorded in ice cores. In the modern Antarctic region, diatoms deplete the ocean in silicic acid Si(OH)₄ to a far greater extent than they do for nitrate NO₃⁻. The addition of iron dramatically lowers the diatom Si(OH)₄:NO₃⁻ uptake ratios, which consequently drives the Antarctic towards NO₃⁻ depletion, with excess Si(OH)₄ remaining in surface waters (Brzezinski et al., 2002). This excess silicic acid is transported northward by oceanic currents to the subtropics where it is integrated into the general equatorial Pacific circulation. The outcome of the “silicic acid leakage” hypothesis is that an excess of Si(OH)₄ would favor the growth of silica-based diatoms at the expense of the calcite-based phytoplankton at low latitudes. Thus, the regional carbonate pump would weaken and the export of organic carbon to the deep seas would increase in the area where this faunal community change happens. A simple box modeling study by Matsumoto et al. (2002) showed that a reduced carbonate pump combined with an open-system carbonate compensation draws down atmospheric pCO₂ from the interglacial 277 p.p.m.v. to 230–242 p.p.m.v. By comparison, a general circulation model with a greater atmospheric pCO₂ sensitivity to [a] reduced carbonate pump combined

with carbonate compensation, [b] reduced global CaCO₃:orgC rain ratio, and [c] an open-system compensation, can reduce atmospheric CO₂ by more than 50 p.p.m. (Archer et al., 2000; Matsumoto et al., 2002).

The “silicic acid leakage” hypothesis predicts that the addition of iron during glacial period in the Antarctic waters should cause a switch from the Si(OH)₄-poor/NO₃⁻-rich state of present day Southern Ocean to a Si(OH)₄-rich/NO₃⁻-poor condition during glacial times (Matsumoto et al., 2002).

Furthermore, the distributions of nutrients in the Pacific are asymmetric about the equator and suggest a critical role for a southern source water, deficient in silicate (Dugdale et al., 2002; Sarmiento et al., 2004). Thus, a positive feedback could exist between the silicate supply from the Southern Ocean and equatorial Pacific diatom productivity (Broecker, 1982; Dugdale et al., 2002; Matsumoto et al., 2002).

Diatom production in the tropics is episodic, depending on silicate availability, in addition to nitrate and phosphate concentrations in the euphotic zone. Diatoms usually dominate the spring blooms in the eastern equatorial Pacific (EEP) (Landry et al., 2000). Consequently, they export CO₂ from the upper ocean and the atmosphere into the deep ocean. If some physical processes continue to supply Si(OH)₄ and nutrients to the surface waters over a long period of time, diatoms can thrive and increase their contribution as efficient CO₂ exporters into the deep ocean and to higher trophic levels (Brzezinski et al., 2002; Matsumoto et al., 2002; Allen et al., 2005).

The tropical Pacific Ocean is a complex environmental system. In the EEP, the predominant controller of the biological productivity is the strength of the westward-blowing Trade Winds. The winds influence the oceanic surface circulation by creating coastal upwelling along South America, which affects the distribution of the chemical fields and the biological processes across the whole EEP. In the Western Pacific Warm Pool (WPWP), a strongly stratified water column prevents the upwelling of cold nutrient-rich water into the euphotic zone. This leads to the formation of a well-mixed warm pool of low biological productivity that mostly responds to ENSO magnitude (Radenac and Rodier, 1996; Beaufort et al., 2001).

In this paper, we first reconstruct the flux of calcite to the seabed as well as the downward flux of organic carbon and combine these fluxes with opal

accumulation rate observations in the equatorial Pacific. Second, we investigate downcore variations in rain ratio and biogenic opal to test for a shift in planktonic community composition and production as predicted by Brzezinski et al. (2002).

2. Oceanography, core location, and stratigraphy

2.1. Oceanography and location

Three cores in the equatorial Pacific were used for this study (Fig. 1 and Table 1). Two cores are located in the EEP and one in the WPWP. Core ODP846B, located just south of the Galapagos Islands, is under the influence of the lower nutrient-rich Equatorial Undercurrent (EUC) and Peru upwelling (Loubere, 2000). Core ODP849B, to the west of core ODP846B, and core MW91–9GCC38 located in the WPWP are under the influence of the water drawn from the equatorial upwelling, fed by the upper nutrient-poor EUC. These differences among the cores reflect two EUC source waters; waters from the North Pacific come in the north equatorial countercurrent (NECC) while waters from the South Pacific come through the New Guinea Coastal Undercurrent (NGCUC) (Toggweiler et al., 1991; Toggweiler and Carson, 1995; Dugdale et al., 2002). All three cores are located above the carbonate compensation depth, far from any hydrothermal sources and from riverine sources of terrigenous material. For all cores, particulate matter sinking through the water column is predominantly biogenic and winds are the only significant supplier of terrigenous material.

2.2. Stratigraphy and new age model

Following work from Skinner and Shackleton (2005) and Loubere and Richaud (unpublished data), it appears that the $\delta^{18}\text{O}$ -based Atlantic stratigraphy leads its Pacific counterpart by about 4000 years. The cause lies with the benthic $\delta^{18}\text{O}$ record, which does not represent a pure sea-level

record (Skinner and Shackleton, 2005). Radiocarbon dates on cores V19–28 (EEP Loubere and Richaud, unpublished data) and TR163–31B (equatorial Pacific; Skinner and Shackleton, 2005) clearly show a 4000-year lag with cores RC13–204 (equatorial Atlantic; Loubere and Richaud, unpublished data) and MD99–2334 K (North Atlantic; Skinner and Shackleton, 2005), respectively, over the LGM through the deglacial time period. After constructing a revised chronology for V19–28 using ^{14}C ages, we correlated the $\delta^{18}\text{O}$ records of the cores used in this study to V19–28's chronology. All core records (Table 2) are adjusted to the calendar timescale of Charles et al. (1996). We were able to construct a revised chronostratigraphy from modern time to about 30,000 calendar years B.P. for cores ODP846B, ODP849B, and MW91–9GCC38. However, we cannot assess with certainty any $\delta^{18}\text{O}$ time lags prior to 30,000 calendar years because of a lack of radiocarbon dating measurements. For all the data relevant to this study between modern time and

Table 1
Core locations

Core	Latitude	Longitude	Water depth (m)
ODP846B	3.095S	90.818W	3307
ODP849B	0.183N	110.517W	3851
MW91–9GCC38	0.005S	159.367W	2456

Table 2
Core chronologies

Core	Proxy	Reference
ODP846B	$\delta^{18}\text{O}$ for <i>Cibicidoides</i> , ^{14}C ages	Mix et al. (1995), Loubere et al. (2007)
ODP849B	$\delta^{18}\text{O}$ for <i>Cibicidoides</i>	Mix et al. (1995)
MW91–9GCC38	$\delta^{18}\text{O}$ for <i>N. dutertrei</i> and <i>G. ruber</i>	Loubere et al. (2007)

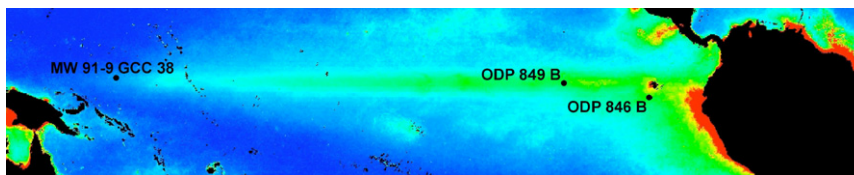


Fig. 1. Core locations in the eastern equatorial Pacific and in the Western Equatorial Pacific. Color gradient represents surface ocean biological productivity. Contours in $\text{gC m}^{-2} \text{yr}^{-1}$.

30,000 calendar years B.P., we used a revised chronostratigraphy (“Revised” Age [cal. ka]), which takes into account the radiocarbon dates. For all older data, we use the timescale of Martinson et al. (1987) (“Old” Age [cal. ka]).

3. Analytical methods

The data used in this article include sediment $^{230}\text{Th}_{x,s}$ activities, calcite and opal percentages, and estimates of calcite and organic carbon fluxes to the seabed.

Sediment calcite percent was determined using a Carlo–Erba NA1500 C/N/S analyzer following the method of Verardo et al. (1990). Samples were calibrated against standard acetanilide and checked against NBS standard reference material 1b (argillaceous limestone). Replicate analyses of the sediments indicate a mean error of $\pm 2\%$ of the estimated calcite value (33 replicates).

Most of the biogenic opal content for cores ODP846B and ODP849B was determined by a single extraction of silica into a Na_2CO_3 solution, following the procedure established by Mortlock and Froelich (1989). Every sample was analyzed twice and the uncertainty is in the order of $\pm 10\%$. Some ODP849B data came from Pichat et al. (2004). In Pichat et al. (2004), the opal content of the sediment was estimated by normative calculations assuming that all the Al is associated with the terrigenous fraction.

Opal preservation for ODP846B and ODP849B was assessed by categorizing into four preservation states the vellum (uniform mesh-like silica microstructure covering the areolae) of the centric diatom *Azpeitia nodulifer*. This provides a relative index of opal preservation at the seafloor (Warnock et al., 2007).

The percent calcite preserved was estimated based on the *Globorotalia menardii* fragmentation index (MFI) of Mekik et al. (2002). This proxy uses a transfer function that calibrates a foraminiferal fragmentation index to biogeochemical model-derived data. The mean error of the transfer function regression is 5.8% (calibration $r^2 = 0.88$ for 38 samples). There is an additional uncertainty in the scaling of the percent preserved calibration estimated to be on the order of $\pm 10\%$. The former is the error estimate for precision, the latter is the potential error in accuracy (Mekik et al., 2002). An average of 140 menardii shells or shell fragments were counted per sample in ODP846B, 530 in ODP849B, and 155 in MW91–9GCC38.

Organic carbon flux is reconstructed using a transfer function that estimates surface ocean biological productivity from assemblages of benthic foraminifera in deep-sea sediments (Loubere and Fariduddin, 1999). There is a strong quantitative relationship between assemblage composition and productivity through the flux of labile organic matter to the seabed. The mean error of the transfer function regression is 10% of estimated value (calibration $r^2 = 0.89$ for 207 samples). The productivity is translated to a seabed flux by using the Jz equation of Berger et al. (1987) ($Jz = [0.17\text{PP}/(z/100)] + 0.01\text{PP}$, where PP is the primary production) This latter step makes for easy comparison of data and is not taken to yield necessarily rigorous benthic fluxes.

The ^{230}Th concentration in sediments was measured by isotope dilution. After acid digestion, the ^{230}Th was extracted from the sediment samples by anion-exchange chromatography (Pichat et al., 2004). Samples from ODP849B and ODP846B were measured by single collector sector-field inductively coupled plasma mass-spectrometry (SF-ICP-MS, Finnigan Element 2) using the technique described by Choi et al. (2001) and Pichat et al. (2004). For core MW91–9GCC38, measurements were made by a multicollector inductively coupled plasma mass-spectrometry (MC-ICP-MS, Nu500—Nu instrument) using multiple ion counting channels with a technique similar to the one described by Thomas et al. (2006). For the SF-ICP-MS measurements, the internal precision was better than 2% (2σ) and the reproducibility for full replicate analyses (dissolution, separation, and spectrometry) was better than 4% (2σ). For MC-ICP-MS measurements, the internal precision was better than 3% and the reproducibility for full replicate analyses was better than 5%. Intercomparison between the two techniques was made by systematically measuring sample ODP849–162 with each batch of sediment. The reproducibility was better than 5% (2σ). Corrections for $^{230}\text{Th}_{x,s}$ were made as explained in Pichat et al. (2004).

Thorium normalization assumes that the flux of ^{230}Th scavenged from the water column (F_{230}) by biogenic and non-biogenic particles is constant and close to its production rate (P_{230}) (Bacon and Rosholt, 1982; Bacon, 1984; Francois et al., 2004). This approximation is justified by the very short residence time of ^{230}Th in the water column, and its validity has been confirmed by models (Henderson et al., 1999) and sediment-trap experiments (Yu et al., 2001). Therefore, the flux of scavenged

$^{230}\text{Th}_{x,s}$ can be used as a reference to estimate the sedimentary flux. A net lateral input of sediment (focusing) will increase the apparent sedimentation rate, and the flux of $^{230}\text{Th}_{x,s}$ will be higher than expected from the vertical input only. Conversely, a net removal of sediment (winnowing) will decrease the apparent sedimentation rate and the flux of $^{230}\text{Th}_{x,s}$ will be lower than the vertical input only. For an extensive description and review of the method, refer to Francois et al. (2004).

The percentages of calcite and opal found in the sediment have been normalized to $^{230}\text{Th}_{x,s}$ in the three cores used in this study when the data were available. For a particular biogenic fraction, the normalization translates as “ ^{230}Th -normalized MAR” for sediment accumulation rates not corrected for preservation, and “ ^{230}Th -normalized vertical flux” for sediment accumulation rates corrected for preservation.

We use (1) a calcite preservation index to obtain a calcite export flux (i.e. export flux = preserved rain rate/fraction calcite preserved) (Mekik et al., 2002), and (2) a quantitative opal preservation proxy to determine the general trend of the opal fluxes (Warnock et al., 2007).

4. Results and discussion

4.1. ^{230}Th -normalized sediment MAR in the equatorial Pacific

The ^{230}Th -normalized sediment accumulation rates of all three cores is presented in Fig. 2. These measurements represent the accumulation of sediment at the seafloor from vertical settling only.

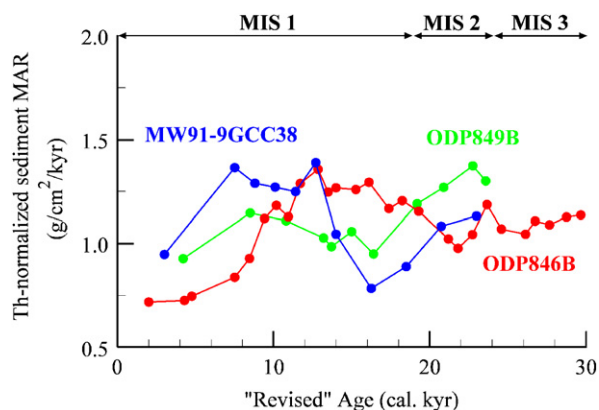


Fig. 2. ^{230}Th -normalized sediment accumulation rates for ODP846B, ODP849B, and MW91-9GCC38. Units are in $\text{g}/\text{cm}^2/\text{kyr}$.

ODP849B and MW91-9GCC38 follow a similar pattern with sediment accumulation decreasing from 24 to 16 cal. ka and increasing between 16 and 8 cal. ka. Values reached around 24 cal. ka are greater than during present, or similar to present, for ODP849B and MW91-9GCC38, respectively. ODP846B experiences a slight increase in sediment accumulation rate from 30 to about 13 cal. ka. From 13 cal. ka to present, its sediment accumulation rate decreases.

4.2. ^{230}Th -normalized calcite mass accumulation rate (MAR) in the equatorial Pacific

The ^{230}Th -normalized calcite accumulation rates of all three cores are shown in Fig. 3. These measurements represent the accumulation of calcite at the seafloor from vertical settling only. Core ODP846B displays a steady increase from 50 to 13 cal. ka and a decrease in calcite accumulation rates from 13 cal. ka to present. The values during MIS 2 (19–24 cal. ka) are lower than during the deglaciation, but higher than during the Late Holocene. Core ODP849B records MIS 2 values higher than deglaciation values and present values. For core MW91-9GCC38, the MIS 2 calcite accumulation rates is lower than those measured for the Late Holocene and for the deglaciation. Also, accumulation rates during Late Holocene (7–10 cal. ka) and deglaciation are similar. Overall, the ^{230}Th -normalized calcite MAR decreases from deglaciation to LGM across the whole equatorial Pacific area. Between 23 and 16 cal. ka, cores MW91-9GCC38 and ODP849B experience a decrease in ^{230}Th -normalized calcite MAR, while the

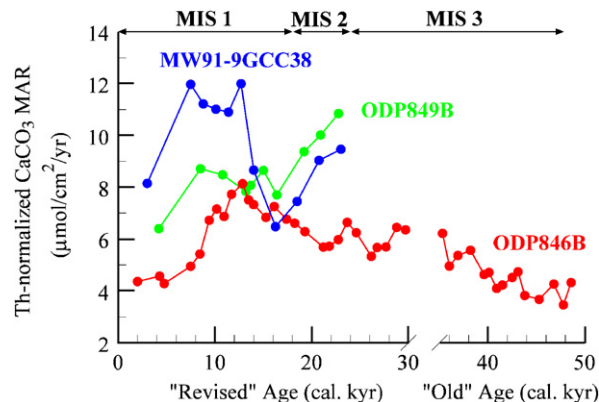


Fig. 3. ^{230}Th -normalized calcite accumulation rates for ODP846B, ODP849B, and MW91-9GCC38. Units are in $\mu\text{mol}/\text{cm}^2/\text{yr}$.

record for core ODP846B continues its increase (Fig. 3).

These results are not consistent with the calcite pattern of deposition found in the EEP by Lyle et al. (2002) during MIS 2. Their calcite accumulation rates, constrained by the more traditional MAR method, are significantly higher during the glacial period than during the Holocene or the deglaciation. As explained in Loubere et al. (2004), sediment redistribution (i.e. focusing) is a significant factor in the increased calcite spike observed by Lyle et al. (2002). An examination of the bathymetry for locations where increased LGM calcite accumulation rates have been inferred shows that all the cores used by Lyle et al. (2002) are in the vicinity of significant topography. Thus, their higher sedimentation rates could represent lateral sediment transport and not production from the upper ocean. Additionally, the recent discovery that the benthic isotope record of the EEP significantly lags the global standard (Skinner and Shackleton, 2005; Loubere and Richaud, unpublished data) leads to a revised chronology that greatly alters MAR estimates, removing the LGM flux peak (Loubere and Richaud, 2007).

4.3. Reconstruction of calcite preservation in the equatorial Pacific

Reconstruction of downcore percent preserved calcite is shown in Fig. 4 using the MFI index of Mekik et al. (2002) (see Methods). For ODP846B and ODP849B, there is a similar trend of decreased preservation from LGM to present. This confirms

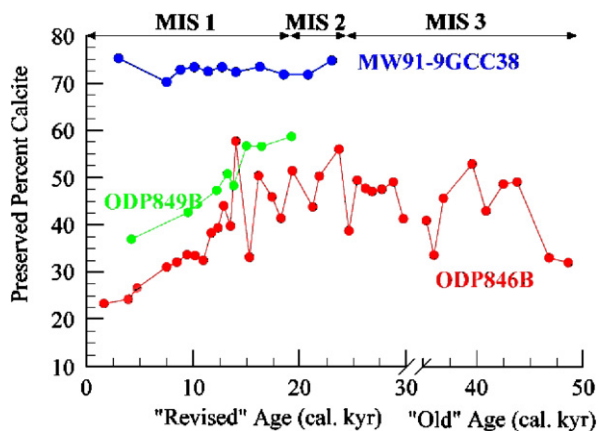


Fig. 4. Preserved calcite percent for ODP846B, ODP849B, and MW91-9GCC38. Units are in %.

that lower Holocene sediment carbonate accumulation rates in the central and eastern equatorial Pacific are mainly driven by increased dissolution (Farrell and Prell, 1989; Stephens and Kadko, 1997). MW91-9GCC38 shows a trend with very little variation between Glacial and present, probably helped in this by its shallower depth compared to the eastern cores (Fig. 4). Similar results from this area are found by Mekik et al. (in preparation).

4.4. Reconstruction of ^{230}Th -normalized calcite vertical flux in the equatorial Pacific

The export fluxes of calcite to the seabed (Fig. 5) were estimated by dividing the $^{230}\text{Th}_{x,s}$ -normalized calcite MAR (Fig. 3) by the fraction of calcite preserved (Fig. 4). The results of all three cores are similar; lowest calcite export fluxes during MIS 2 and highest calcite export fluxes during the Holocene. Note that ODP846B records an export calcite flux similar to ODP849B despite its location within the influence of the Peru upwelling system.

4.5. Preserved opal accumulation rates in the equatorial Pacific

The ^{230}Th -normalized opal accumulation rates present a very different picture across the equatorial Pacific (Fig. 6) than ^{230}Th -normalized calcite MAR (Fig. 3) or ^{230}Th -normalized calcite vertical flux (Fig. 5). These measurements represent the accumulation of opal at the seafloor from vertical settling only. Cores ODP849B and MW91-9GCC38

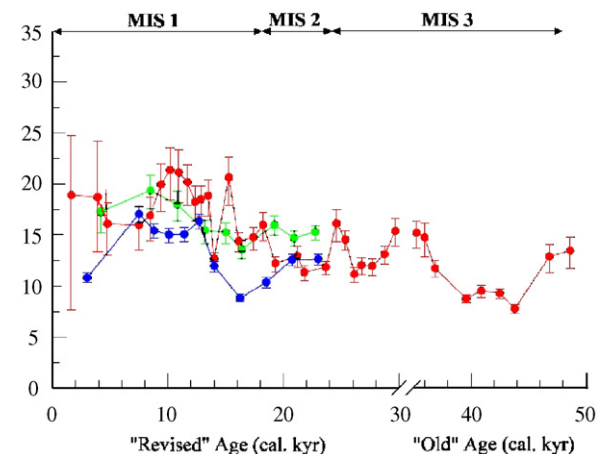


Fig. 5. ^{230}Th -normalized calcite vertical flux to the seabed for ODP846B, ODP849B, and MW91-9GCC38. Units are in $\mu\text{mol}/\text{cm}^2/\text{yr}$.

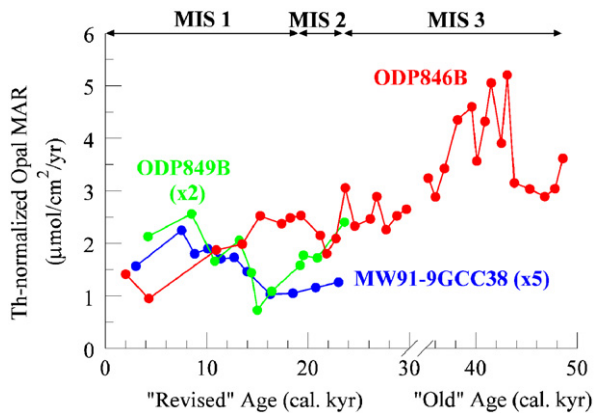


Fig. 6. ^{230}Th -normalized opal accumulation rates for ODP846B, ODP849B, and MW91-9GCC38. Units are in $\mu\text{mol}/\text{cm}^2/\text{yr}$.

show a similar pattern, with decreasing opal accumulation rates for the period 24–16 cal. ka, then increasing accumulation rates from 16 cal. ka to present. Core ODP846B shows a steady decreasing pattern from mid-MIS 3 to present.

It is difficult to assess opal preservation as there is no quantitative proxy for this available thus far. However, opal preservation records for ODP846B and ODP849B have been developed by Warnock et al. (2007) using the vellum (uniform mesh-like silica microstructure covering the areolae) of the centric diatom *A. nodulifer*. The vellum was categorized into four preservation states, providing a relative index of opal preservation at the seafloor.

At location ODP849B, better preservation is observed between 3 and 9 cal. ka and between 18 and 22 cal. ka than during the period 11–16 cal. ka (Warnock et al., unpublished data). This suggests that the decrease recorded during MIS 2 could reflect the imprint of decreasing surface production rather than increase in dissolution at the seafloor (Fig. 6). Similarly, the increase in opal accumulation rates from 14 cal. ka to present also could reflect increased surface production of diatoms rather than a decrease in dissolution at the seafloor (Fig. 6). At location ODP846B, the decrease in opal accumulation rate during MIS 3 (Fig. 6) was not accompanied by improved preservation. In fact, glacial preservation at this core appears similar to that of the Holocene (Warnock et al., 2007). Thus, the opal accumulation rate appears primarily driven by production at the surface ocean, making it likely that opal surface production decreased from MIS 3 toward present in core ODP846B.

4.6. Comparison of the calcite and opal preserved rain rates with the surface ocean productivity

We assembled the calcite record (Fig. 5), the opal record (Fig. 6), and a record from a benthic foraminiferal transfer function tracking the flux of orgC to the seafloor (see Methods) for ODP846B (Fig. 7).

As explained in Loubere and Fariduddin (1999), there is a strong quantitative relationship between benthic foraminifera assemblage composition and productivity through the flux of labile organic matter to the seabed. Thus, the benthic foraminifera record is actually a proxy for downward labile organic matter flux to the seabed. From 42 cal. ka to present, the productivity displays a pattern with smaller scale variations (Fig. 7), indicating a quasi-constant flux of organic carbon to the seafloor. By contrast, calcite paleo-flux drops significantly through MIS 3 and 2. In MIS 1 and 2, we observe a clear association between orgC and calcite fluxes, where increase (decrease) in productivity is matched by increase (decrease) in calcite flux to the seabed. In stage 3, where opal accumulation rates are higher, we see calcite flux generally inverse to opal accumulation rate while orgC flux varies modestly.

4.7. Comparison of the opal preserved rain rate with the ratio flux index

The orgC/ CaCO_3 flux ratio for ODP846B (Fig. 8) was produced by dividing the reconstructed orgC flux to the seabed (Fig. 7) by the ^{230}Th -normalized

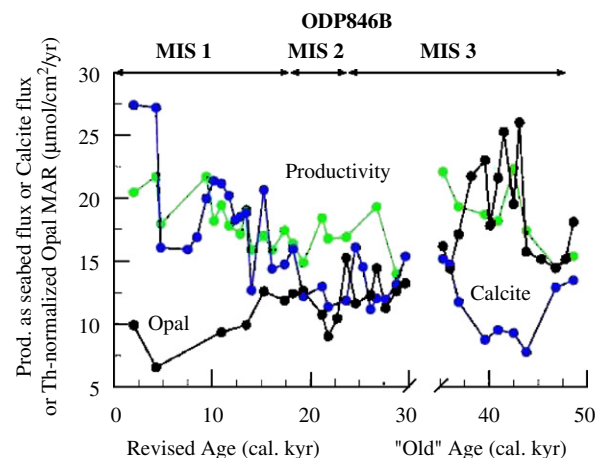


Fig. 7. Reconstruction of calcite flux to the seabed, surface ocean productivity, and preserved opal rain rate for ODP846B. Units are in $\mu\text{mol}/\text{cm}^2/\text{yr}$.

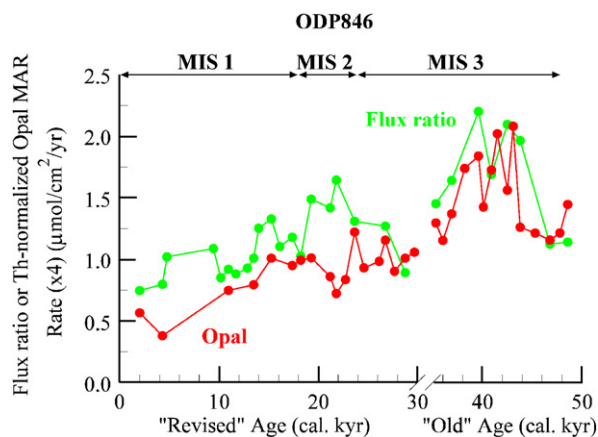


Fig. 8. OrgC/CaCO₃ flux ratio and ²³⁰Th-normalized opal accumulation rate for ODP846B. Units are in µmol/cm²/yr.

calcite vertical flux (Fig. 5). The ²³⁰Th-normalized opal accumulation rate is from Fig. 6.

There is a clear match between the flux ratio and the preserved opal rain rate, and both records vary concomitantly. This indicates that the flux ratio was variable in time and that its decrease can be associated to lower opal fluxes from MIS 3 to MIS 1. It likely denotes the floral shift anticipated by the “silicic acid leakage” hypothesis. The calcite-based planktonic community increases in importance from MIS 3 to MIS 2 (Fig. 5) while the silica-based planktonic community diminishes during the same periods (Fig. 6). These results have implications for the transport of labile organic carbon to the seabed in the EEP. Work by Francois et al. (2002) and Klaas and Archer (2002) as well as Armstrong et al. (2001) show that ballasting plays an important role in this process. Calcium carbonate is seen as the most effective mineral phase to transport organic matter deepest in the water column. The coupling of calcite flux to orgC transport is supported by our results between 25 cal. ka and present (Fig. 7). However, during MIS 3 we find peaks in orgC flux also associated with higher opal accumulation rates (Fig. 7). This, along with the coherent shifts in reconstructed rain ratio that we observe, indicates that a ballasting system shifted to the opal mineral phase can still lead to elevated orgC transport to depth. Nevertheless, it may be that surface productivity was higher in MIS 3 than we estimate using benthic foraminifera due to a decrease in orgC transport efficiency as the plankton community became more diatom rich.

5. Conclusions

Our data indicate an elevated flux ratio throughout MIS 2 and 3. This implies a weakened carbonate pump and a stronger silica pump. Our data also indicate that organic carbon flux to depth is not simply a function of calcium carbonate fluxes, but is clearly responsive to diatom production. Our results from core ODP846B, which is under the influence of the Peru upwelling, support a faunal displacement as hypothesized by Brzezinski et al. (2002), where the growth of diatoms was favored at the expense of the calcite-based phytoplankton by an excess of Si(OH)₄ transported from the sub-antarctic. This particularly applies to MIS 3.

Our results provide evidence that changes in calcite fluxes across the whole equatorial Pacific are fairly simple and consistent. For all three cores used in this study, the correction of ²³⁰Th-normalized calcite accumulation rates with a proxy for percent calcite preserved yield a glacial calcite export flux lower than during the Late Holocene, and this despite the cores being located in different oceanographic settings. Indeed, ODP849B and MW91–9GCC38 are under the influence of the equatorial divergence, and ODP846B is under the influence of the Peru margin upwelling.

²³⁰Th-normalized opal accumulation rates show a different picture. ODP846B is the only core that experiences a peak in opal accumulation rates starting during MIS 3 and declining toward the LGM. This decrease occurred while the opal preservation index is about constant throughout the record—indicating that the increase is not related to preservation state but related to surface production. Thus, opal accumulation rates from the surface were likely greater than would be inferred from the sediments. The decrease during MIS 2 and 3 of the opal flux is concomitant with a significant increase in the calcite export flux. ODP849B, the other core with opal preservation data, shows better preservation during the LGM and the Holocene than during the deglacial. This provides evidence for lower opal surface production during deglaciation and the Early Glacial in the equatorial divergence band. Thus, we find evidence for higher opal production in the area most influenced by Peru upwelling, where the subantarctic connection is strongest. This result follows the observations of Loubere (2000) and Loubere et al. (2003) showing that biogeochemical responses differ between the Peru upwelling and equatorial divergence systems.

Finally, the $\text{orgC}/\text{CaCO}_3$ flux ratio mirrors the ^{230}Th -normalized opal accumulation rates for ODP846B. This shows the displacement of the calcite-based community by a silica-based community during MIS 2 and MIS 3. This only occurs in the area subjected to the Peruvian upwelling influence and not in the area under the influence of the equatorial upwelling. Our results provide support for decreased silica leakage from mid-MIS 3 to the Early Glacial. Its influence seems restricted to the eastern part of the EEP where diatom production was highest during MIS 3. Since we did not observe a peak of opal flux at the LGM, we conclude that there was no silicic acid leakage during MIS 2. Moreover, it is difficult to assert the influence of the silicic acid leakage during MIS 3 on the low CO_2 concentrations prevalent at the time.

Acknowledgements

This research was partially supported by American Chemical Society Grant no. 39527-AC2. Our mass spectrometer facilities were developed with the aid of a major instrumentation grant from the National Science Foundation. We thank core curators at Oregon State University (June Padman, Bobbi Conard) and the Ocean Drilling Program for their assistance in sampling cores. M.R. has been supported by research assistantships through P.L. For S.P., this research has been supported by a Marie Curie Fellowship of the European Community programme Improving the Human Research Potential and the Socio-Economic Knowledge Base under contract number HPMF-CT-2002-02068.

References

- Allen, J., Brown, L., Sanders, R., Moore, M., Mustard, A., Fielding, S., Lucas, M., Rixen, M., Savidge, G., Hensen, S., Mayor, D., 2005. Diatom carbon export enhanced by silicate upwelling in the Northeast Atlantic. *Nature* 437 (29), 728–732.
- Archer, D., Winguth, A., Lea, D., Mahowald, N., 2000. What caused the glacial/interglacial atmospheric $p\text{CO}_2$ cycles? *Reviews of Geophysics* 38 (2), 159–189.
- Armstrong, R., Leea, C., Hedges, J., Honjoc, S., Wakeham, S., 2001. A new, mechanistic model for organic carbon fluxes in the ocean based on the quantitative association of POC with ballast minerals. *Deep-Sea Research II. Topical Studies in Oceanography* 49, 219–236.
- Bacon, M., 1984. Glacial to interglacial changes in carbonate and clay sedimentation in the Atlantic Ocean estimated from ^{230}Th measurements. *Isotope Geosciences* 2, 97–111.
- Bacon, M., Rosholt, J., 1982. Accumulation rates of ^{230}Th , ^{231}Pa , and some transition metals on the Bermuda Rise. *Geochimica et Cosmochimica Acta* 46 (4), 651–666.
- Beaufort, L., de Garidel-Thoron, T., Mix, A., Pisias, N., 2001. ENSO-like forcing on oceanic primary production during the Late Pleistocene. *Science* 293, 2440–2444.
- Berger, W., Fisher, K., Lai, C., Wu, G., 1987. Ocean productivity and organic carbon flux. Part I. Overview and maps of primary production and export production. Technical Report reference series pp. 30–87.
- Boyd, P., Watson, A., Law, C., Abraham, E., Trull, T., Murdoch, R., Bakker, D., Bowie, A., Buesseler, K., Chang, H., 2000. A mesoscale phytoplankton bloom in the polar Southern Ocean stimulated by iron fertilization. *Nature* 407, 695–702.
- Broecker, W., 1982. Ocean chemistry during glacial time. *Geochimica et Cosmochimica Acta* 46, 1689–1705.
- Brzezinski, M., Pride, C., Franck, M., Sigman, D., Sarmiento, J., Matsumoto, K., Gruber, N., Rau, R., Coale, K., 2002. A switch from $\text{Si}(\text{OH})_4$ to NO_3^- depletion in the glacial Southern Ocean. *Geophysical Research Letters* 29, 5.
- Buesseler, K., Andrews, J., Pike, S., Charette, M., 2004. The effects of iron fertilization on carbon sequestration in the Southern Ocean. *Science* 304 (5669), 414–418.
- Charles, C., Lynch-Stieglitz, J., Ninnemann, U., Fairbanks, F., 1996. Climate connections between the hemisphere revealed by deep sea sediment core/ice core correlations. *Earth and Planetary Science Letters* 142 (1–2), 19–27.
- Choi, M., Francois, R., Sims, K., Bacon, M., Brown-Leger, S., Flier, A., Ball, L., Schneider, D., Pichat, S., 2001. Rapid determination of ^{230}Th and ^{231}Pa in seawater by desolvated-micronebulization inductively-coupled magnetic sector mass spectrometry. *Marine Chemistry* 76, 99–112.
- Coale, K., Johnson, K., Fitzwater, S., Gordon, R., Tanner, S., Chavez, F., Ferioli, L., Sakamoto, C., Rogers, P., Millero, F., Steinberg, P., Nightingale, P., Cooper, D., Cochlan, W., Landry, M., Constantinou, J., Rollwagen, G., Trasvina, A., Kudela, R., 1996. A massive phytoplankton bloom induced by an ecosystem-scale iron fertilization experiment in the equatorial Pacific Ocean. *Nature* 383, 495–501.
- Dugdale, R., Wischmeyer, A., Wilkerson, F., Barber, R., Chai, F., Jiang, M., Peng, T., 2002. Meridional asymmetry of source nutrients to the equatorial Pacific upwelling ecosystem and its potential impact on ocean–atmosphere CO_2 flux; a data and modeling approach. *Deep-Sea Research II* 49, 2513–2531.
- Farrell, J., Prell, W., 1989. Climatic change and CaCO_3 preservation: an 800,000 year bathymetric reconstruction from the central equatorial Pacific Ocean. *Paleoceanography* 4, 447–466.
- Francois, R., Honjo, S., Krishfield, R., Manganini, S., 2002. Factors controlling the flux of organic carbon to the bathypelagic zone of the ocean. *Paleoceanography* 16 (4), 1087.
- Francois, R., Frank, M., Rutgers van der Loeff, M., Bacon, M., 2004. ^{230}Th -normalization: an essential tool for interpreting sedimentary fluxes during the Late Quaternary. *Paleoceanography* 19 (PA1018).
- Henderson, G., Heinze, C., Anderson, R., Winguth, A., 1999. Global distribution of the ^{230}Th flux to ocean sediments constrained by GCM modelling. *Deep-Sea Research I* 46, 1861–1893.
- Klaas, C., Archer, D., 2002. Association of sinking organic matter with various types of mineral ballast in the deep sea:

- implications for the rain ratio. *Global Biogeochemical Cycles* 16 (4), 1116.
- Landry, M., Constantinou, J., Latasa, M., Brown, S., Bidigare, R., Ondrusek, M., 2000. Biological response to iron fertilization in the eastern equatorial Pacific (IronEx II). III. Dynamics of phytoplankton growth and microzooplankton grazing. *Marine Progress Series* 201, 57–72.
- Loubere, P., 2000. Marine control of biological production in the eastern equatorial Pacific Ocean. *Nature* 406, 497–500.
- Loubere, P., Fariduddin, M., 1999. Quantitative estimation of global patterns of surface ocean biological productivity and its seasonal variation on time scales from centuries to millenia. *Global Biogeochemical cycles* 13, 115–133.
- Loubere, P., Richaud, M., 2007. Some reconciliation of glacial–interglacial calcite flux reconstructions for the eastern equatorial Pacific. *Geochemistry Geophysics Geosystems* 8, Q03008 [doi:10.1029/2006GC001367].
- Loubere, P., Fariduddin, M., Murray, R., 2003. Patterns of export production in the eastern equatorial Pacific over the past 130,000 years. *Paleoceanography* 18 (2), 1028.
- Loubere, P., Figen, M., Francois, R., Pichat, S., 2004. Export fluxes of calcite in the eastern equatorial Pacific from the Last Glacial Maximum to present. *Paleoceanography* 19, 2018.
- Loubere, P., Richaud, M., Mireles, S., 2007. Variability in tropical thermocline nutrient chemistry on the glacial/interglacial timescale. *Deep-Sea Research II*, this issue [doi:10.1016/j.dsr2.2007.01.005].
- Lyle, M., Mix, A., Pisias, N., 2002. Pattern of CaCO₃ deposition in the eastern tropical Pacific Ocean for the last 150 kyr: evidence for a southeast Pacific depositional spike during Marine Isotope Stage (MIS) 2. *Paleoceanography* 17 (2), 1013.
- Martinson, D., Pisias, N., Hays, J., Imbrie, J., Moore, T., Shackleton, N., 1987. Age dating and the orbital theory of the ice ages: development of a high resolution 0–300,000 year chronostratigraphy. *Quaternary Research* 27, 1–29.
- Matsumoto, M., Sarmiento, J., Brzezinski, M., 2002. Silicic acid leakage from the southern Ocean: a possible explanation for glacial atmospheric CO₂. *Global Biogeochemical Cycles* 5.
- Mekik, F., Loubere, P., Archer, D., 2002. Organic carbon flux and organic carbon to calcite flux ratio recorded in deep-sea carbonates; demonstration and a new proxy. *Global Biogeochemical Cycles* 16 (3), 1052.
- Mekik, A.F., Ridgwell, A., François, R., Loubere, P., Richaud, M., in preparation. Is carbonate compensation from the last deglaciation responsible for the gradual increase in atmospheric CO₂ during the holocene?
- Mix, A., Le, J., Shackleton, N., 1995. Benthic foraminiferal stable isotopes stratigraphy of site ODP846: 0–1.8 Ma. In: *Proceedings of the Ocean Drilling Program—Scientific Results*, vol. 138, pp. 839–854.
- Mortlock, R., Froelich, P., 1989. A simple method for the rapid determination of biogenic opal in pelagic marine sediments. *Deep-Sea Research II* 36 (9).
- Palmer, M., Pearson, P., 2003. A 23,000-year record of surface water pH and pCO₂ in the western equatorial Pacific Ocean. *Nature* 300, 480–482.
- Petit, J., Jouzel, J., Raynaud, D., Barkov, N., Barnola, J., Basile, I., Bender, M., Chappellaz, J., Davis, M., Delaygue, G., Delmotte, M., Kotlyakov, V., Legrand, M., Lipenkov, V., Lorius, C., Pepin, L., Ritz, C., Saltzman, E., Stievenard, M., 1999. Climate and atmospheric history of the past 420,000 years from the Vostok ice core Antarctica. *Nature* 399, 429–436.
- Pichat, S., Sims, K., Francois, R., McManus, J., Leger, S., Albarede, F., 2004. Lower export production during glacial periods in the equatorial Pacific derived from ²³¹Pa/²³⁰Th measurements in deep-sea sediments. *Paleoceanography* 19 (4), 21.
- Radenac, M.H., Rodier, M., 1996. Nitrate and chlorophyll distributions in relation to thermocline and current structures in the western tropical Pacific during 1985–1989. *Deep-Sea Research II* 43 (4–6), 725–752.
- Sarmiento, J., Gruber, N., Brzezinski, M., Dunne, J., 2004. High-latitude control of thermocline nutrients and low latitude biological productivity. *Nature* 427, 56–60.
- Sigman, D., Boyle, B., 2000. Glacial/Interglacial variations in atmospheric carbon dioxide. *Nature* 407, 859–869.
- Skinner, L., Shackleton, N., 2005. An Atlantic lead over Pacific deep-water change across Termination I: implications for the application of the marine isotope stage stratigraphy. *Quaternary Science Reviews* 24, 571–580.
- Stephens, M., Kadko, D., 1997. Glacial–Holocene calcium carbonate dissolution at the central equatorial Pacific seafloor. *Paleoceanography* 12, 797–804.
- Takahashi, T., Sutherland, S., Sweeney, C., Poisson, A., Metz, N., Tilbrook, B., Bates, N., Wanninkhof, R., Feely, R., Sabine, C., Olafsson, J., Nojiri, Y., 2002. Global sea-air CO₂ flux based on climatological surface ocean pCO₂, and seasonal biological and temperature effects. *Deep-Sea Research II* 49, 1601–1622.
- Thomas, A., Henderson, G., Robinson, L., 2006. Interpretation of the ²³¹Pa/²³⁰Th paleocirculation proxy: new water-column measurements from the southwest Indian Ocean. *Earth and Planetary Science Letters*.
- Toggweiler, J., Carson, S., 1995. What are upwelling ecosystems contributing to the ocean's carbon and nutrient budgets? In: Summerhayes, C., Emeis, K., Angel, M., Smith, R., Zeitschel, B. (Eds.), *Upwelling in the Ocean, Modern Processes and Ancient Records*. Wiley, New York, pp. 337–361.
- Toggweiler, J., Dixon, D., Broecker, W., 1991. The Peru upwelling and the ventilation of the South Pacific thermocline. *Journal of Geophysical Research* 96, 20467–20497.
- Verardo, D., Froelich, P., McIntyre, A., 1990. Determination of organic carbon and nitrogen in marine sediment using the Carlo Erba NA–1500 analyzer. *Deep-Sea Research* 37 (1), 157–165.
- Warnock, J., Scherer, R., Loubere, P., 2007. A quantitative assessment of diatom dissolution and late Quaternary primary productivity in the Eastern Equatorial Pacific. *Deep-Sea Research II*, this issue [doi:10.1016/j.dsr2.2007.01.011].
- Yu, E., Francois, R., Bacon, M., Fleer, A., 2001. Fluxes of ²³⁰Th and ²³¹Pa to the deep sea: implications for the interpretation of excess ²³⁰Th and ²³¹Pa/²³⁰Th profiles in sediments. *Earth and Planetary Science Letters* 191, 219–230.